




Article

Phytoremediator Potential of *Ipomea asarifolia* in Gold Mine Waste Treated with Iron Impregnated Biochar

Hercília Samara Cardoso Costa ¹, Edna Santos de Souza ², Yan Nunes Dias ^{1,*} , Leônidas Carrijo Azevedo Melo ³  and Antonio Rodrigues Fernandes ¹ 

¹ Institute of Agricultural Sciences, Federal Rural University of Amazon (ICA-UFRA), Belém 66077-830, Brazil; herciliacosta23@gmail.com (H.S.C.C.); antonio.fernandes@ufra.edu.br (A.R.F.)

² Xingu Institute of Studies, Federal University of the South and Southeast of Pará (UNIFESPA), São Félix do Xingu 68380-000, Brazil; edna.souza@unifesspa.edu.br

³ Department of Soil Science, Federal University of Lavras (UFLA), Lavras 37200-000, Brazil; leonidas.melo@ufla.br

* Correspondence: yanynd1@gmail.com

Abstract: Growing environmental pollution in recent decades has been generating potentially toxic elements (PTE) which pose an ongoing threat to terrestrial and aquatic ecosystems and human health, especially in mining areas. Biochar and PTE-tolerant species have been used in soil remediation as they are environmentally friendly alternatives. This study aimed to assess the influence of açai seed biochar (*Euterpe oleracea* Mart), impregnated with iron (BFe) or not (BC), on the bioavailability of PTEs, in a multi-contaminated soil from a gold (Au) mining area in the Amazon, using *Ipomea asarifolia* as a plant test since it was naturally growing on the tailings. BC increased the soil pH while BFe reduced. Biochars increased PTEs in the oxidizable fraction (linked to soil organic matter). The use of BC and BFe improved the immobilization of PTEs and BC increased arsenic (As) in the easily soluble fraction in the soil. Moreover, plants grown with biochars showed lower dry matter yield, higher concentrations of PTEs and lower nutrient content than the control treatment. According to the phytoextraction and translocation factors, *Ipomea asarifolia* can be classified as a species with potential for phytostabilization of Zn and tolerant to other PTEs, mainly As.

Keywords: Cachoeira do Piriá; remediation; multi-contaminated soils; tolerance to metals; biochar



Citation: Costa, H.S.C.; de Souza, E.S.; Dias, Y.N.; Melo, L.C.A.; Fernandes, A.R. Phytoremediator Potential of *Ipomea asarifolia* in Gold Mine Waste Treated with Iron Impregnated Biochar. *Minerals* **2022**, *12*, 150. <https://doi.org/10.3390/min12020150>

Academic Editor: Jaume Bech

Received: 1 December 2021

Accepted: 25 January 2022

Published: 26 January 2022

Publisher's Note: MDPI stays neutral with regard to jurisdictional claims in published maps and institutional affiliations.



Copyright: © 2022 by the authors. Licensee MDPI, Basel, Switzerland. This article is an open access article distributed under the terms and conditions of the Creative Commons Attribution (CC BY) license (<https://creativecommons.org/licenses/by/4.0/>).

1. Introduction

Potentially toxic elements (PTEs) are naturally present in the environment. However, human activities, such as mining, have considerably increased the concentrations of these elements in ecosystems [1]. Waste piles from mining activities normally contain high levels of PTEs that contribute to environmental pollution [2–4]. The residues generated in artisanal mining are usually randomly deposited in areas with large extension, constituting a source of dispersion of contaminants, which can reach water bodies, vegetation and enter the food chain from aqueous medium or via soil particles, through runoff, leaching, and volatilization and methylation (e.g., Hg) [3–5].

Due to persistence in the environment, mobility, and speciation, PTEs can be transferred and accumulated in the food chain, resulting in adverse effects on physiological and biochemical processes in plants and soil microorganisms [6,7]. In addition, PTEs can be accumulated in vital organs of the human body, leading to a potential danger to the health of those who live in the vicinity of mining areas [8]. The material resulting from the processing of ores is highly erodible, lacking nutrients and physical structure, in addition to having reduced microbial biodiversity [9,10]. For the recovery of areas degraded by mining and with high levels of PTEs, several strategies have been developed, such as the use of biochar or modified biochar associated with phytoremediator species [5].

Biochar stands out as an efficient soil conditioner and consists of a carbon-rich byproduct of the thermochemical decomposition of organic material generated in the absence or limited supply of oxygen [11]. The chemistry of biochar surface is complex and contains several functional groups that give acidic (mainly provided by carboxyl and hydroxyl) and basic (mainly provided by groups with O and N and some minerals such as CaO, MgO, and CaCO₃) characteristics [12]. They also have hydrophilic and hydrophobic properties according to the type of organic material and pyrolysis conditions [13].

Biochar is also a promising adsorbent for the remediation of contaminated soils, due to its high capacity to retain organic and inorganic species [14]. The high adsorption capacity is linked to its high specific surface, porosity, and diversity of functional groups [12,15]. Biochar can also improve soil fertility, as it provides nutrients, increases organic matter, and favors microbial activity, in addition to reducing the availability of PTEs, enhancing plant growth [1].

Chemical, physical, and biological modification methods have been proposed which aim to increase the adsorption capacity and expand biochar application in the remediation of various contaminants [16]. This modification results in changes in the specific surface area, porosity, cation/anion exchange capacity, functional surface groups, and pH [17,18]. For instance, iron (Fe) impregnation in biochar has been efficient in removing arsenate (H₂AsO₄⁻) and dichromate (Cr₂O₇²⁻) from aqueous solution, since the positive charges of oxidized Fe allows an increase in the anion exchange capacity [19,20].

Several techniques have been developed to remediate contaminated soils (chemical oxidation/reduction, washing, electrokinetic restoration, chemical extraction, and stabilization), but most of these conventional methods have high cost, little practicality and do not contribute to improving chemical, physical, and biological soil attributes [21–24]. Phytoremediation is an alternative and unexpensive method to immobilize PTEs, which consists of using plant species that have adaptive mechanisms to accumulate or tolerate high concentrations of contaminants in their rhizosphere [25,26]. However, soils with high available concentrations of PTEs, low fertility and poor structure can compromise the success of phytoremediation, as they inhibit revegetation [9]. Therefore, the use of soil amendments such as biochar can contribute to the success of phytoremediation.

Biochar application in contaminated soils, associated with phytoremediator species, can guarantee greater success in soil remediation programs [1,15,18]. The species used in this study belongs to the family Convolvulaceae (*Ipomoea asarifolia*) and can be found throughout the study area in Cachoeira do Piriá, state of Pará. Because it is a native plant and has the ability to grow in contaminated soils, it may have improved efficiency when associated with biochar in the recovery of soils contaminated by PTEs. Açai (*Euterpe oleracea* Mart) seed biochar, impregnated with iron (BFe) or not (BC), was studied in the bioavailability of PTEs in multicontaminated soil from a gold mining area (Au) in the Amazon, cultivated with *Ipomea asarifolia*.

2. Materials and Methods

2.1. Description of the Study Area

Mining waste was collected in a gold mining area located in the municipality of Cachoeira do Piriá (01°45'35" S, 46°32'42" W). The municipality of Cachoeira do Piriá has a territorial extension of approximately 2419 km² and belongs to the microregion of Guamá, in the northeastern region of Pará, Eastern Amazon (Figure 1) [27]. The climate is equatorial (Af) according to the Köppen classification. The average annual precipitation can reach 3000 mm, with a dry or less rainy period (July to December) and a rainy period (January to June). The average annual temperature varies between 26 and 30 °C.

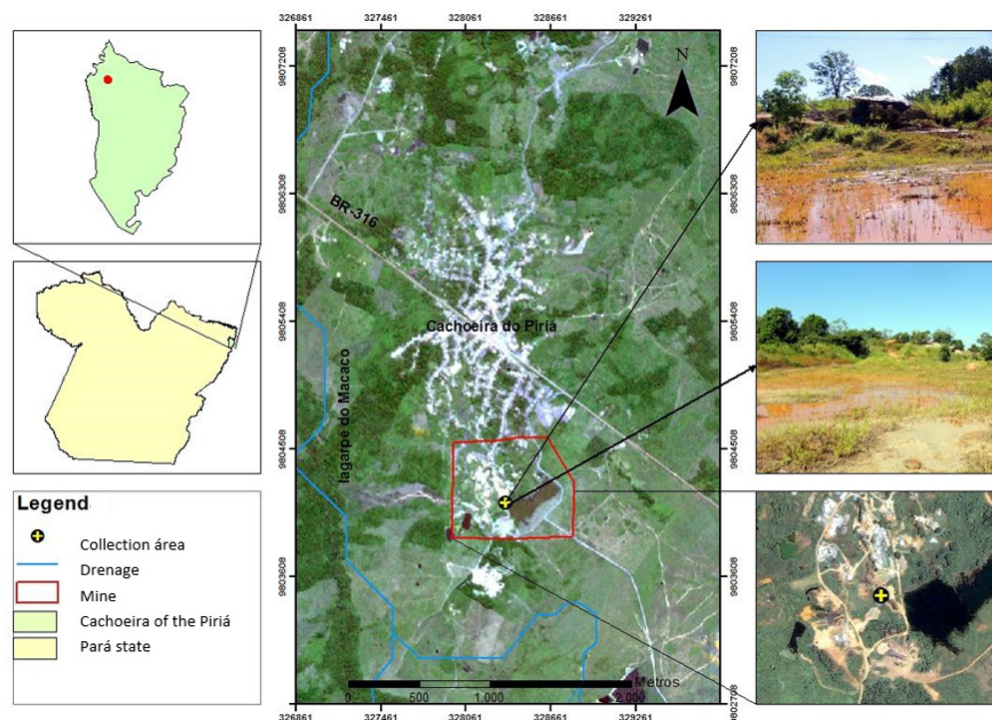


Figure 1. Location of the collection area in the municipality of Cachoeira do Piriá, Pará.

The artisanal mining area is located in the lower Gurupi-Proterozoic formation. The supracrustal sequence is composed of mafic, metamorphic, metavolcanic, and intrusive rocks, and basic composition metatuffs. Most of these lithologies were marked by processes of hydrothermal and supergenic alteration [28] and produced a relatively constant mineralogical composition of quartz, dolomite, chlorite, albite, arsenolite, bearsite, alar-site, sericite, and sulfide [29]. The mineral products are mainly pyrite, arsenopyrite, and arsenic oxide, and minor amounts of galena, sphalerite, chalcopyrite, and gersdorffite with a geochemical association of the elements Au, Ag, and As [30]. The region was marked by the exploration of gold (Au), tin (Sn), and copper (Cu) [31]. The gold rush started in the 1980s by attracting miners and companies, currently gold mines have moved towards the exploration of Au present in primary deposits and this advance is made possible through excavations that reach more than 140 m. Cyanidation pools and Hg are used to recover the Au as an amalgam of Au [32].

The municipality has an estimated population of 33,900 inhabitants and the main economic activities are agriculture, livestock, subsistence fishing and mainly mining [27]. Due to mineral exploration, the region is marked by the intense removal of soil that led to the formation of several pits and areas with surface modified by excavations, as well as the accumulation of waste and sterile material [31]. In places of intense exploration, the removal of soil and processing of rocks give rise to large piles with high levels of PTEs. The piles are formed by the mixture of sterile, waste and soil, which was called contaminated mine soil (SC) for the purpose of this study and was used in the experiment.

2.2. Soil Sampling and Characterization

Samples of the contaminated material and secondary vegetation/forest soil (SM) were collected in the 0.0–0.2 m layer. The soil of SM (without contamination) was collected in Belém, Pará, under the coordinates 48°26'14" W and 1°27'22" S and 9 m altitude, with climate classified as Af according to the Köppen classification and average temperature of 26 °C. After collection, the samples were air-dried, homogenized, passed through 2-mm sieve and stored in polyethylene recipients. The granulometric analysis was performed using the pipette method, with NaOH as a chemical dispersant and mechanical agitation

for 16 h. The clay fraction was separated by sedimentation, the sand by sieving and the silt was calculated by difference [33].

The chemical attributes were quantified according to Embrapa [33]. The pH in water was determined at a soil:water ratio of 1:2.5. Calcium (Ca^{2+}), magnesium (Mg^{2+}), and aluminum (Al^{3+}) were extracted with KCl 1 mol L^{-1} ; Ca^{2+} and Mg^{2+} were quantified by titration with $0.0125 \text{ mol L}^{-1}$ EDTA, and Al^{3+} by titration with 0.025 mol L^{-1} NaOH. The available phosphorus (P) and potassium (K) were extracted with Mehlich-1 solution (0.05 mol L^{-1} HCl + $0.0125 \text{ mol L}^{-1}$ H_2SO_4); K was quantified by flame photometry and P by colorimetry. Potential acidity (H + Al) was obtained by calcium acetate (pH 7) method and determined by titration with 0.025 mol L^{-1} NaOH. Organic carbon was obtained by oxidizing organic matter using a potassium dichromate solution in the presence of sulfuric acid (Walkley–Black procedure), and the soil organic matter (SOM) content was obtained by multiplying the organic carbon content by a factor of 2.0 [34].

The pseudo-total contents of PTEs were extracted by the method EPA 3051A, using 0.5 g of soil (passed through a $150 \mu\text{m}$ sieve) and 9 mL of HNO_3 + 3 mL HCl [35]. The concentrations of As, Co, Cr, Cu, Hg, Ni, Mn, Pb, Ba, Fe, and Al were quantified by inductively coupled plasma optical emission spectrometry (ICP-OES). The analysis was performed in duplicate, with blank samples and certified reference material (144 ERM-CC141) in each battery. The relative standard deviation was calculated, resulting in approximately 10% for most elements of the certified samples.

2.3. Production and Impregnation of Biochar

The biochar was produced from açai (*Euterpe oleracea* Mart) seeds, which are a residue generated during the processing of the açai fruit. The seeds were washed and dried at room temperature, then they were pyrolyzed at $700 \text{ }^\circ\text{C}$ for 1 h, with a heating rate of $4 \text{ }^\circ\text{C}/\text{min}$, in a muffle furnace with controlled temperature and slow cooling to room temperature, using 100 g of seeds per closed crucibles. The temperature of $700 \text{ }^\circ\text{C}$ was chosen based on the Cu and Zn adsorption capacity of the biochar [12].

The Fe impregnation was carried out by adding the biochar in a $0.1 \text{ M FeCl}_3 \cdot 6\text{H}_2\text{O}$ solution and ultrapure water at a ratio of 1:15 (g mL^{-1}) biochar/solution, followed by stirring on a mechanical stirrer for 24 h. The pH was maintained between 4.5 and 5 (1.0 mol L^{-1} HCl or NaOH for adjustment) to increase the solubility of Fe and incorporation into the biochar matrix. Then, the samples were washed with ultrapure water to remove the non-adsorbed Fe and dried in an oven at a constant temperature of $60 \text{ }^\circ\text{C}$ for 48 h [19].

2.4. Characterization of Biochar

The pH and electrical conductivity (EC) were determined at a ratio of 1:10 (solid: solution, *w/v*) [10]. The cation exchange capacity (CEC) was measured using the ammonium acetate (NH_4OAc) method [36]. In 40 mL of 1.0 mol L^{-1} NH_4OAc , 0.1 g of biochar was added in a 50 mL polyethylene tube and stirred for 20 min, then it was filtered. Subsequently, it was washed with 30 mL of isopropanol, followed by addition of 40 mL of 1.0 mol L^{-1} KCl. The NH_4^+ contained in the KCl solution was quantified using the salicylate colorimetric method [37]. Prior to soil CEC determination, the soil was washed with deionized water and the biochar was washed with 0.1 mol L^{-1} HCl to remove excess salts [38]. The determination of soil CEC after the experiment followed the same methodology, but with 1.0 g of soil sample.

The pseudo-total contents of PTE were determined by acid digestion in a microwave oven, with 0.5 g of the material placed in Teflon tubes and digested with hydrochloric acid (HCl) and nitric acid (HNO_3) in the proportion of 1:3 (aqua regia). Quantification was performed using ICP-MS. All samples were analyzed in triplicates, with reagent blank (no soil). The point of zero charge (PZC) was estimated according to Yang et al. [39], in which 60 mg of biochar was added to 20 mL of 0.01 mol L^{-1} CaCl_2 solutions at pH 2, 4, 6, 8, and 10 (previously adjusted with HCl and 0.1 mol L^{-1} NaOH), followed by stirring for 24 h in a horizontal shaker and equilibrium pH measurement.

2.5. Greenhouse Experiment

A greenhouse experiment was carried out using polyethylene pots containing 2 kg of the mixture of contaminated soil, secondary vegetation soil and biochars in different proportions (*w/w*) (Tables 1 and 2). The experimental design was in randomized blocks, with seven treatments and four replicates. For SM + SC mixture, the proportion of 50% (SM/SC) of each soil was used [9]. The pots with treatments were incubated for 60 days, with humidity maintained at 70% by water replacement by weight weekly.

Table 1. Chemical properties of the soils used in the experiment.

	Sand	Clay	Silt	^a CEC	^b OM	pH
	g kg ⁻¹			cmol kg ⁻¹	g kg ⁻¹	H ₂ O
^c SC	340.1	46.8	613.1	47.6	8.3	8.3
^d SM	538	330	132	76.1	12.6	4.6

^a Cation exchange capacity (pH 7); ^b Organic matter; ^c Contaminated soil; ^d secondary vegetation/forest soil.

Table 2. Identification for treatments according to the mixture of contaminated mine soil (SC), forest soil (SM), biochar (BC) and biochar impregnated with Fe (BFe).

Treatments	Identification
Control: contaminated soil (100%)	TC-SC
Control: forest soil (100%)	TC-SM
Contaminated soil (50%) + forest soil (50%)	SC + SM
Contaminated soil (50%) + forest soil (45%) + biochar (5%)	SC + SM + BC
Contaminated soil (50%) + forest soil (45%) + biochar Fe impregnated (5%)	SC + SM + BFe
Contaminated soil (95%) + biochar (5%)	SC + BC
Contaminated soil (95%) + biochar Fe impregnated (5%)	SC + BFe

The plant species used was *Ipomoea asarifolia* due to the potential of the genus in phytoremediation programs [40–42], and also due to its abundant presence in the tailing piles of the study area (Cachoeira do Piriá municipality). The collected plants were grown in a greenhouse and then replicated by cuttings for seedling production for the experiment. A seedling of *Ipomoea asarifolia* with two fully expanded leaves per pot was used, and cultivation was carried out for 110 days with daily water replacement, in order to keep humidity at 70%.

2.6. Soil Analysis after the Experiment

Soil pH and EC were measured in a 1:2.5 soil/solution ratio [1] and chemical analyses (Ca, K, Mg available, and P) were performed according to Embrapa [33]. Metal fractionation was carried out by sequential extraction following the European Community Bureau of Reference method to verify the mobility of PTEs after the experiment. The fractions were operationally divided into: exchangeable fraction (F1) extracted with 0.11 mol L⁻¹ acetic acid; reducible fraction (F2), obtained with 0.5 mol L⁻¹ hydroxylamine hydrochloride (pH 1.5—adjusted with HNO₃); oxidizable fraction (F3), extracted by digestion in hydrogen peroxide, followed by the addition of 1 mol L⁻¹ ammonium acetate (pH 2.0—adjusted with HNO₃) [43]. The residual fraction (F4) was obtained by the difference between the total levels and the sum of the other fractions. The pseudo-total contents of PTEs were extracted by the acid digestion method in a microwave oven [35]. The elements Ba, Cd, Co, Cu, Cr, Fe, Pb, Ni, Mn, S, and Zn in all fractions were measured using an inductively coupled plasma optical emission spectrometer—ICP-OES. For quality control assurance, a reference material (ERM-CC141—loam soil) and blank reagents were used in each extraction batch. The relative standard deviation was calculated, and this was approximately 10% for most elements of the certified samples.

The arsenic fractionation followed the method developed by Drahotka et al. [44], which establish the following fractions: soluble As (F1); arsenates adsorbed to amorphous min-

erals (F2); arsenates bound to crystalline minerals (F3); well-crystalline arsenates, oxides, and hydroxosulfates of Fe (F4); as well as sulfides and arsenides (F5). F1 was obtained by extraction with ultrapure water (1:25 *m/v*), after 10 h shaking; the F2 was obtained with 0.01 mol L⁻¹ ammonium phosphate, after 16 h shaking (1: 100 *m/v*); the F3 was extracted with 0.2 mol L⁻¹ ammonium oxalate (in the dark, pH 3, stirred for 2 h); the F4 was extracted with 0.2 mol L⁻¹ ammonium oxalate (pH 3, for 4 h, at 80 °C); and the F5 determined by acid digestion in a microwave oven, with 0.5 g of the material placed in Teflon tubes and digested with KCl/HCl/HNO₃ solution (1/1/1 ratio). As concentration in all fractions was determined by inductively coupled plasma optical emission spectrometer—ICP-OES. The fractionation of metals and As was performed in duplicate and included blank reagents and a certified soil sample (ERM-CC141—loam soil) in each batch. The relative standard deviation was calculated, and this was approximately 5% of the certified samples.

2.7. Plant Analyses

Plants were harvested after 110 days of cultivation, washed with deionized water and shoots and roots were separated. At harvest, samples of fresh and photosynthetically active leaves were separated and stored in a freezer at -80 °C for analysis of chlorophylls and carotenoids. The rest of the material was kept for 48 h at a constant temperature of 60 °C in a forced ventilation oven. Then, the dry weight was obtained by grinding the material in a stainless mill for further analysis.

The total content of chlorophyll and carotenoids was obtained according to Lichtenthaler [45]. Fresh leaves were extracted from 0.1 g of homogenized leaf tissue in the presence of CaCO₃ and 5 mL of 80% acetone. The obtained extract was placed in a 25 mL conical flask and the volume was made up with ultrapure water. An aliquot was removed and the photosynthetic pigments were measured by absorbance of light at 470, 646.8, and 663.2 nm by spectrophotometer.

The contents of PTEs in plants were obtained by acid digestion in a microwave oven. For this, 2.0 mL of HNO₃ + 2 mL of H₂O₂ and 5 mL of ultrapure water were added in 0.25 g of oven-dried plant material [4]. All samples were evaluated in triplicate and the quality control of the analyses was performed with samples of the reference material ERM-CD281 (rye grass) and reagent blank in each batch. The relative standard deviation was calculated, and this was approximately 8% for most elements. The levels of elements in the extracts were determined by inductively coupled plasma optical emission spectrometer—ICP-OES.

2.8. Bioconcentration and Translocation Factors

To assess the phytoremediation potential, the bioconcentration factor (BCF) (Equation (1)) and the translocation factor (TF) (Equation (2)) were calculated for each element [46]. BF represents the plant efficiency in absorbing PTEs from the soil, while TF indicates the plant ability to translocate an element from root to shoot.

$$\text{Bioconcentration factor} = \left[\frac{\text{root concentration (mg/kg)}}{\text{soil concentration (mg/kg)}} \right] \quad (1)$$

$$\text{Translocation factor} = \left[\frac{\text{shoot concentration (mg/kg)}}{\text{root concentration (mg/kg)}} \right] \quad (2)$$

2.9. Statistical Analysis

To check the abnormal distribution of the data, the Shapiro–Wilk normality test was performed. The concentrations of the elements were log transformed in order to normalize the data distribution. Descriptive analysis was performed to determine measures of central tendency and variability. The data were submitted to ANOVA and the averages were compared using the Tukey test ($p < 0.05$) using R 4.1.0 software (R Core Team 2021).

3. Results and Discussion

3.1. Characterization of Biochar

The pH of the BC was high (9.9) and that of the BFe was low (2.7) (Table 3). The high pH of BC is due to the formation of Ca, Mg and oxyhydroxide carbonates during the pyrolysis process, especially at relatively high temperature (700 °C) [47]. Conversely, the low pH of Bfe may be due to the ion exchange that occurs between basic cations on the biochar surface and Fe ions during the impregnation [48], which agrees with a marked reduction in the biochar pH from 10.7 to 4.8 after impregnation with Fe observed by Yin et al. [19]. We also observed a considerable reduction in basic cations (Ca + K + Mg) from 9.0 g kg⁻¹ in the BC to 3.1 g kg⁻¹ in the Bfe, and an increase in Fe content (acid cation) from 0.9 g kg⁻¹ in the BC to 9.6 g kg⁻¹ in the Bfe (Table 3), which corroborates the ion exchange process during impregnation and washing processes.

Table 3. Characterization of biochars.

	Ca	K	Mg	P	Fe	^a EC	^b CEC	^c PZC	pH _{H2O}
	g kg ⁻¹					μS cm ⁻¹	cmolc kg ⁻¹		
^d BC	1	7.2	0.8	2	0.9	1655	127.3	7.6	9.9
^e Bfe	0.5	2.1	0.5	1.3	9.6	1620	105.1	3.6	2.7

^a Electrical conductivity; ^b Cation exchange capacity; ^c Point of Zero Charge; ^d Biochar not impregnated; ^e Biochar impregnated with Fe. (Average values followed by standard deviation).

The PZC decreased from 7.6 in the BC to 3.6 in the Bfe (Table 3), which may be due to the formation of Fe oxides on the surface of the biochar that generate acid compounds [48] and/or the oxygenation of functional groups such as –COOH and –SO₂OH, giving rise to a biochar of acidic nature [49]. PZC is an important indicator of the net surface load and shows the preference of a sorbent for ionic species [46]. When the pH of the medium is greater than the PZC value, it means that the negative charged sites dominate, while the pH of the medium is lower than the sorbent positive charges dominate [50].

The impregnation process (Bfe) provided a decrease in the concentrations of K, P, Ca, and Mg (71, 50, 35, and 38%, respectively) in relation to BC (Table 3). There was an increase in Fe concentration in the BFe of approximately 10 times when compared with the BC, which was lower when compared with other Fe impregnation studies that observed increases of 47 [46], 147 [51], and 10 [52] times. The efficiency of Fe impregnation depends mainly on the solution pH, solubility of the Fe source, oxidizing agent, Fe impregnation before or after pyrolysis [53], as well as material characteristics and production temperature [12].

Biochars showed high CEC. BFe's CEC decreased by 17% compared to BC, even so it remained high (Table 3). This suggests that the negative charge sites were reduced, increasing the positive charges and consequently the immobilization capacity of anionic pollutants. Biochars normally have high CEC due to the potentially high content of functional groups and high specific surface [12,18,54] in addition to the pH that influences variable amount of soil charge, and with the increase it promotes the elevation of CEC [55]. In soil with high CEC, it reduces the leaching of nutrients from the soil profile and increases the availability of nutrients to the roots of plants, favoring the immobilization of cationic pollutants [46].

3.2. Biochar Effect on Soil Attributes

Most soil chemical reactions are influenced by soil pH, such as the solubility of PTEs [56,57]. BC addition significantly increased the pH of SC, while BFe addition reduced slightly (from 7.8 to 7.5), even at an application rate of 5% (Table 4). The reduction of the pH of alkaline soil from mining with biochar might favor the development of plants and microorganisms [1] and improve the revegetation of these areas. Conversely, a pH increase in alkaline soils might cause the solubilization of anionic PTEs (e.g., As) [58]. The alkalinity of biochar is shown to be effective in immobilizing cationic metals, especially in acidic soils [17], which occur in more unstable and exchangeable forms [3,59]. Melo et al. [47]

evaluated the effect of sugarcane straw biochar on the Cd and Zn sorption capacity in two acidic tropical soils (pH of 5.7 and 5.2) and observed an increase in the sorption of both metals and a marked increase in the equilibrium soil pH after biochar amendment.

Table 4. Chemical attributes of the soil after experiment.

	^a pH	^b EC	^c CEC
	H ₂ O	μS cm ⁻¹	cmolc kg ⁻¹
SC	7.8 b ± 0.07	55.0 c ± 0.17	48.4 f ± 0.55
SM	4.6 f ± 0.07	19.2 c ± 0.19	77.0 a ± 2.73
SC + SM	6.8 d ± 0.17	51.2 c ± 0.07	58.5 d ± 0.87
SC + SM + BC	7.8 b ± 0.04	376.2 b ± 0.46	79.1 a ± 1.23
SC + SM + BFe	6.4 e ± 0.07	163.4 a ± 0.05	65.3 bc ± 0.88
SC + BC	8.7 a ± 0.08	209.2 c ± 0.41	77.3 ab ± 1.95
SC + BFe	7.5 c ± 0.07	75.6 b ± 0.03	64.7 bc ± 0.91

^a pH in H₂O; ^b Electrical conductivity; ^c Cation exchange capacity. Values with the same letter are not significant by the Tukey test ($p < 0.05$). SC = contaminated soil, SM = forest soil, SC + SM = contaminated soil + forest soil, SC + SM + BC = contaminated soil + forest soil + biochar, SC + SM + BFe = contaminated soil + forest soil + biochar Fe impregnated, SC + BC = contaminated soil + biochar, SC + BFe = contaminated soil + biochar Fe impregnated. (Mean values ± standard deviation).

Both BFe and BC addition increased soil EC up to 7-fold when compared with the control soils (SM and SC), reaching 376 μS cm⁻¹ in the SC + SM + BC treatment (Table 5). The increase in soil EC is related to the soluble salts from a nutrient-rich BC [12], which are hydrolyzed and increase the EC of the solution [19]. Lebrun et al. [9] found a three-fold increase in EC when applying wood biochar to mine soil. High soil EC levels can affect plant growth by interfering in water potential and accumulation of solutes in plant cells [59]. Conversely, at adequate levels, soil EC allows ionic balance, favoring plant growth. Therefore, biochar characteristics and application rate must be chosen carefully to create better conditions for plant growth in contaminated areas.

Table 5. Content of potentially toxic elements in gold mining soil in Cachoeira do Piriá, Pará.

	As	Ba	Co	Cr	Cu	Hg	Ni	Mn	Pb	Zn	Fe	Al
	mg kg ⁻¹						g kg ⁻¹					
Forest soil	-	0.05	-	0.2	0.07	-	0.02	0.21	-	9.90	0.07	0.15
Mine soil	3760	70	58.6	569	121	0.99	454	1280	34.2	112.05	125	7.1
^a QRV	1.4	14.3	-	24.1	9.9	0.26	1.4	72	4.8	7.2	7.1	5.9
^b Prevention	15	150	25	75	60	0.5	30	-	72	300	-	-
^b Investigation	35	300	35	150	200	12	70	-	180	450	-	-

^a Quality Reference Values (Fernandes et al., 2018) [60]; ^b Conama (2009) [61].

3.3. Biochar Affects the Mobility of PTEs

In treatments with the addition of BC and BFe, the Co content was reduced in the exchangeable and reducible fraction (Figure 2A). In the control (SC), the exchangeable fraction corresponded to 6% of the pseudo-total content, while in SC + BC and SC + BFe, the values decreased to 3 and 4%, respectively. Cobalt in the oxidizable fraction increased 65% in SC + BC and 15% in SC + BFe, compared to SC. The treatments that received BC had a higher OM content, which increases the negative charges, and the pH was higher than the PZC (Table 3), indicating that there is a predominance of negative charges on the surface [46]. In soils with a predominance of negative charges, there is a greater adsorption of metallic cations [15], resulting in a reduction of Co mobility. It is noteworthy that with the increase of Co in the oxidizable fraction (linked to OM), unstable organometallic compounds can occur, which can make it again bioavailable [19].

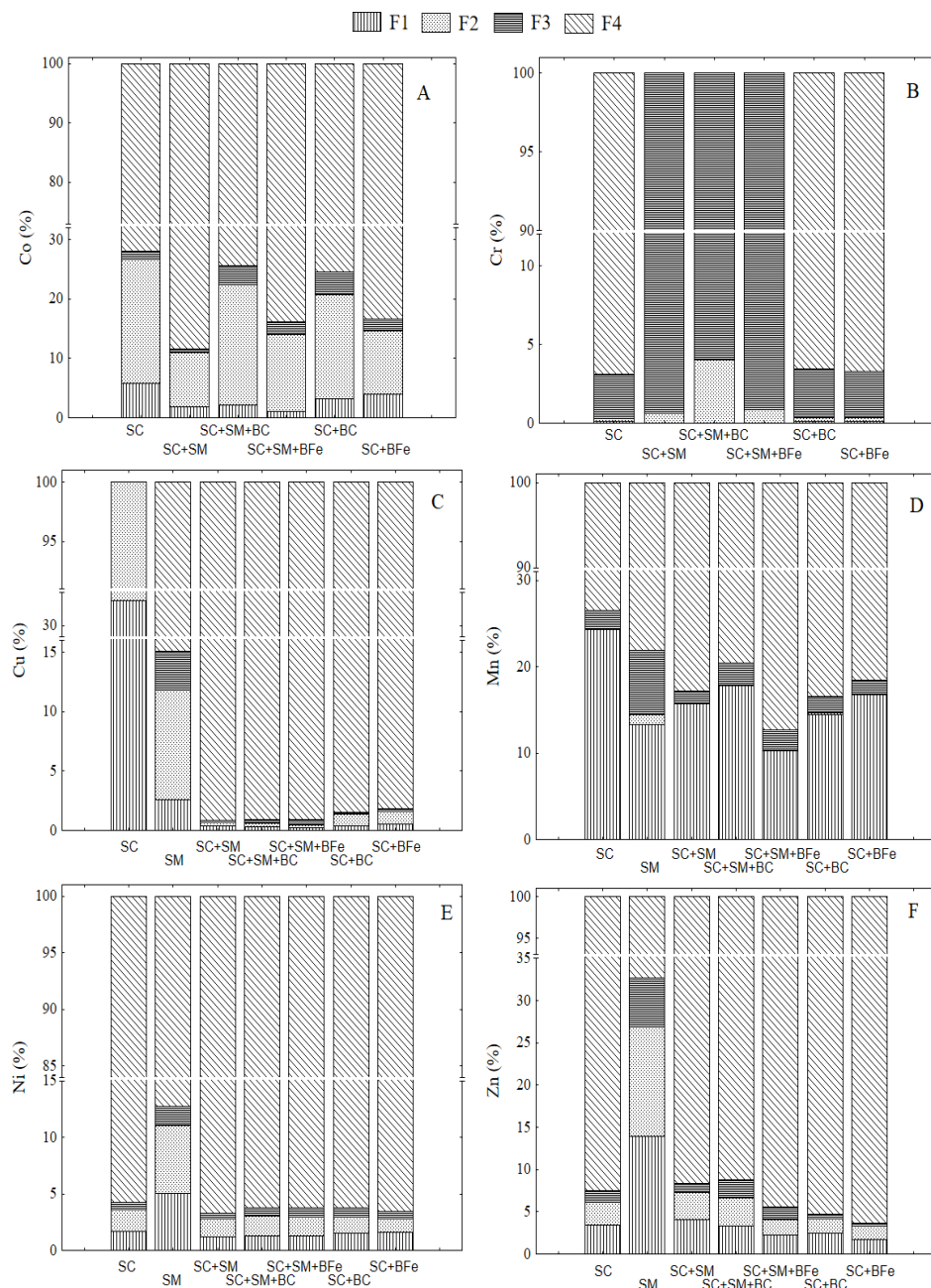


Figure 2. Fractionation of Co (A), Ni (B), Cu (C), Cr (D), Mn (E), and Zn (F) in the soil after the experiment. Exchangeable fraction (F1), linked to exchangeable cations and carbonates, reducible fraction (F2), linked to oxides and hydroxides of Fe and Mn; oxidizable fraction (F3), complexed by organic matter and sulfides; and residual fraction (F4), associated with silicate minerals. SC = contaminated soil, SM = forest soil, SC + SM = contaminated soil + forest soil, SC + SM + BC = contaminated soil + forest soil + biochar, SC + SM + BFe = contaminated soil + forest soil + biochar Fe impregnated, SC + BC = contaminated soil + biochar, SC + BFe = contaminated soil + biochar Fe impregnated.

The concentrations of Cu and Zn decreased in the exchangeable and reducible fractions with the addition of biochars (Figure 2C,F). However, it was observed that Cu increased and Zn decreased in the oxidizable fraction, compared to SC. In SC, the pseudo-total content of Cu and Zn were 105.5 and 105.7 mg kg⁻¹ (Table 4), respectively, however, due to the greater affinity of Cu for OM [4], there was a greater increase of this element in the oxidizable fraction compared to Zn. In a study with isotherms and wood biochar, Ressa et al. [62] obtained the following decreasing sequence of affinity Pb > Cu > Cd ≥ Zn >

Ni. Souza et al. [3] found a strong and negative correlation between exchangeable Cu and OM ($r = -0.9$) and a positive correlation ($r = 0.9$) between the availability of Zn and OM, suggesting that the biochar and organic waste used decreased the availability of Cu and increased that of Zn.

The pseudo-total levels of Mn in the studied soils are in the range of 22.5 to 1070 mg kg⁻¹ (SC) (Table 4). Of this total, relatively high levels were obtained in the exchangeable fraction (24%) in SC. With the addition of biochars, decreases occurred in the exchangeable fraction and mainly in the reducible fraction, with the latter being reduced by 40 and 46% in SC + BC and SC + BFe, respectively compared to SC. The application of biochar changed important attributes that made it possible to change Mn in these fractions, such as the increase in OM, CEC and pH. In soil, Mn is commonly found in the form of Mn²⁺ and its solubility is reduced by pH above 6. In addition, it can be found in association with organic and inorganic compounds [63].

The use of biochar did not alter the mobility of Cr in SC, which was low, remaining more than 96% in the residual fraction and the majority remaining in the oxidizable fraction (Figure 2B). Cr in soils with pH > 6 predominates in the form of Cr (OH)²⁺, it is easily adsorbed on the soil by the specific adsorption mechanism [64]. In soils that have neutral or alkaline pH, there is low availability of some PTEs, such as Cr. However, in soils (tailings) exposed as occurs in the mining areas of this study, the pH may become acidic over time, due to the loss of bases, resulting from the action of biotic and abiotic factors and thus favoring the presence of PTEs in exchangeable forms, which may increase ecological and human health risks [65].

Ni (Figure 2E) showed a behavior similar to Cr, being predominant in the residual fraction (>95%) in all treatments, except for SM. The increase in pH is one of the main mechanisms that increase the immobilization of PTEs, due to the application of biochar to the soil [65]. The characteristics of biochar, such as the high specific surface and functional surface groups, also favor the reduction of the availability of PTEs by ion exchange, complexation, precipitation, and adsorption phenomena [18]. In addition, biochar degradation releases organic acids that can easily complex PTEs, resulting in low solubility organic compounds [1,57].

3.4. Effect of Biochars on Arsenic Mobility

Biochar has been used effectively to remove PTEs in soils [52,64], mainly in acidic soils. However, some PTEs generally occur in anionic form in the environment, which limits adsorption, for example As in the biochar. In order to increase the number of specific adsorption sites, Fe-enriched materials have been used in the soil, due to their large surface area and high reactivity, which favor the anion adsorption [44,66].

Organometallic compounds can be very stable or easily soluble, depending on several factors in the soil, such as pH, redox potential, OM content and type of metal/metalloid [19,52,67]. In SC, As predominated in the form of sulfides and arsenates (F5) (91.7%), while 7.8% was distributed in the adsorbed fractions (F2) and linked to amorphous and poorly crystallized oxides and Fe hydroxides (F3) (Figure 3). In the F2 and F3 fractions, the percentage was low, but the concentrations were extremely high (133.6 and 127.5 mg kg⁻¹, respectively) (Figure 3). The highest As content linked to the residual fraction demonstrates the high affinity for minerals and reflects the predominant mineral composition in the area, mainly arsenopyrite and arsenic oxide [30]. In these fractions, As is potentially dissolved and can be absorbed by plants.

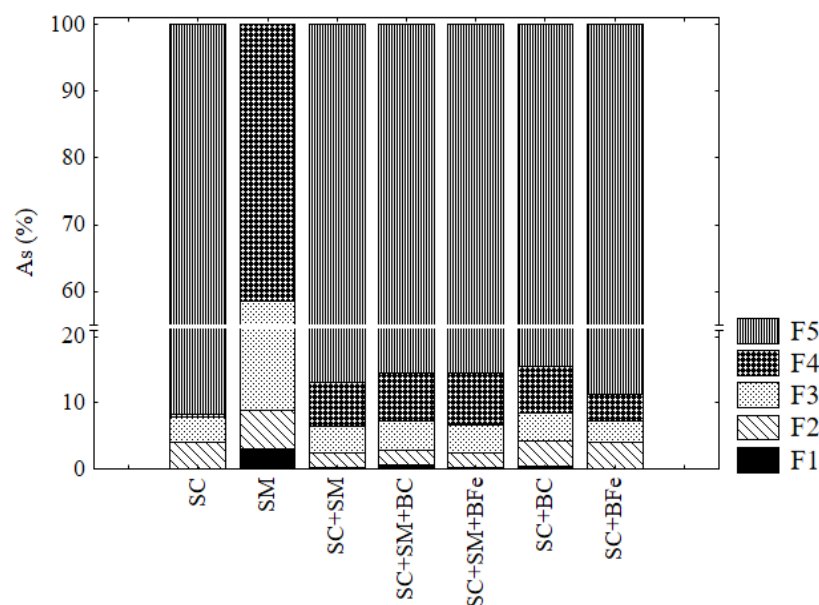


Figure 3. Fractionation of arsenic (As) in the soil after the experiment. F1: easily soluble; F2: adsorbed; F3: bound to amorphous and poorly crystallized Fe oxides and hydroxysulfates; F4: well-crystalline arsenates, oxides, and hydroxosulfates of Fe; F5: sulfides and arsenides. SC = contaminated soil, SM = forest soil, SC + SM = contaminated soil + forest soil, SC + SM + BC = contaminated soil + forest soil + biochar, SC + SM + BFe = contaminated soil + forest soil + biochar Fe impregnated, SC + BC = contaminated soil + biochar, SC + BFe = contaminated soil + biochar Fe impregnated.

The addition of biochars altered fractions of As in the soil, but the predominance remained in the form of sulfides and arsenates (F5) (86%), followed by As associated with amorphous and well-crystallized Fe oxides and hydroxysulfates (F3 and F4, respectively), except for SC + BFe, which occurred in F2 and F3. With SC + BC, the exchangeable fraction decreased from 4 to 3.8%, and increased F3 from 3.8 to 4.2% and F4 from 0.5 to 7.1%. In the SC + BFe treatment, there was a reduction in the mobility of As, compared to SC, in F2 (3.78 for 3.14%), and an increase in F4, which is a more stable fraction (0.51 to 1.65%). The more mobile fraction (soluble) decreased (0.11 to 0.08%), while it increased in the treatment with SC + BC (0.11 to 0.39%).

In fractions F2 and F3, As accumulates on the surface of oxyhydroxides and clay minerals containing Fe and Al and hydroxysulfates [51]. Such fractions are the most important environmentally, because they have high mobility, thus representing an environmental risk for the surrounding area [44]. In soil with alkaline pH, adsorption of As is high due to the formation of Fe (Fe (OH)₃) hydroxides, which can be precipitated as insoluble compounds from ion exchange [52] as well as reaction exchange of Fe (OH)₃ and As, forming complexes with single or bidentate ligand [48].

The increase of As concentration in the more stable fractions (F3 and F4) is due to the increase in pH, OM and surface functional groups, containing organic and mineral components, which increase the surface binders in the soil [38]. Whereas in alkaline soils As (III) is predominant, there is less repulsion with hydroxyl, favoring electrostatic interactions and precipitation in more stable forms [68]. At a high pH, Fe (Fe (OH)₃) hydroxides are easily formed on the surface of biochar, favoring the precipitation of As with Fe³⁺, from ion exchange [48]. Arsenic has a strong attraction for Fe and can bind to amorphous and crystalline Fe oxides, which justifies the accumulation in these fractions [69]. The accumulation in fractions F3 and F4 decreases the mobility of As and, consequently, the environmental risk.

When Fe was incorporated into the biochar (SC + BFe), there was an increase in As associated with amorphous and well crystallized Fe oxides and hydroxysulfates, respectively, due to the large surface area and high Fe reactivity [70], which increase the number

of specific adsorption sites, changing the pH (at the point of zero charge), which promotes electrostatic interactions between As and the adsorbent surface [70]. Increased As associated with Fe oxides in contaminated soil, treated with rice straw biochar impregnated with FeCl_2 , was observed by Yin et al. [19]. The addition of biochar, impregnated with Fe to contaminated alkaline soil, caused the reduction of adsorbed As and the increase of As linked to amorphous and well crystallized oxides and hydroxysulfates [52].

The increase in the bioavailability of As for the more soluble fractions, when biochar was added (SC + BC), may be due to the increase in OM, which in turn favors microbial growth, which consumes oxygen and decreases the redox potential more quickly, favoring solubilization [71]. The organic acids from the dissolved carbon can also contribute to the increase in the Fe (II) solution, through the reductive dissolution of iron oxides, releasing As [51,59]. In addition, the treatments had an alkaline nature, thus, the basic character of these soils associated with the high PZC of BC resulted in a negative net charge on the surface of the biochar, reducing the adsorption of As. The addition of biochar also increased P in the soil, which is likely to the increase in the mobility of As through competitive adsorption/desorption reactions [59,72].

3.5. Effect of Biochars on Plant Biomass

The addition of both BC or BFe did not influence the production of dry matter ($p < 0.05$), either when mixed with forest soil (SM) or not (Figure 4). The only exception was the SC + BC treatment, in which there was a reduction in both root or shoot biomass due to the excess increase in soil pH (from 7.8 to 8.7), soil EC (from 55 to 202 $\mu\text{S cm}^{-1}$), and As solubility (F1 + F2). Under high soil EC, energy is reduced to minimize oxidative stress and there is lower nutrient uptake, due to high ionic competition in the root zone [1]. The accumulation of salts in soil promotes a reduction in the soil water potential, which causes physiological disturbances, including a reduction in the photosynthetic activity, leading to lower biomass yield [73]. Exposure to high concentrations of As results in deleterious effects on plants, such as physiological, morphological, and biochemical disorders, including reduced elongation, number of leaves and leaf area, inhibiting photosynthesis and biomass accumulation [74].

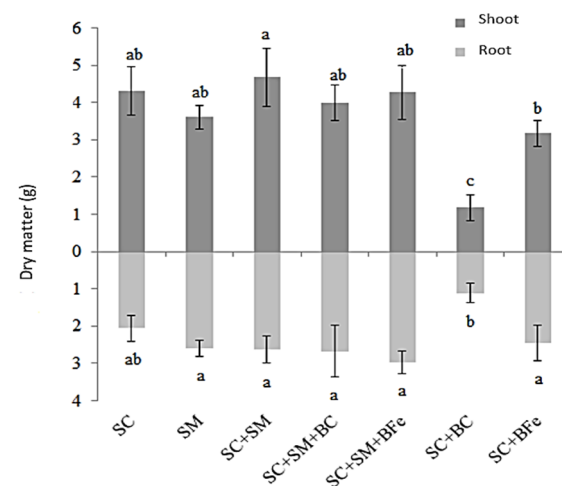


Figure 4. Dry matter of shoot and root of *Ipomoea asarifolia*. SC = contaminated soil, SM = forest soil, SC + SM = contaminated soil + forest soil, SC + SM + BC = contaminated soil + forest soil + biochar, SC + SM + BFe = contaminated soil + forest soil + biochar Fe impregnated, SC + BC = contaminated soil + biochar, SC + BFe = contaminated soil + biochar Fe impregnated. Mean values with standard deviation bars. Values with the same letter are not significant by the Tukey test ($p < 0.05$), $n = 4$.

Biochars, in general, reduced the PTE content of the exchangeable fraction, but increased PTE in the oxidizable fraction (linked to OM). Organic carbon and water-soluble phenolic compounds help to release PTEs from the oxidizable fraction [19,66]. The high con-

concentrations in plants, as well as the increase of PTEs in the oxidizable fraction of SC + BC, suggest that the elements adsorbed, complexed, or precipitated on organic carbon were solubilized, favoring the absorption by the roots (Figure 4).

The concentrations of As in plants exceed the reference values of As for most species (Table 6). Arsenic values in the range between 0.1 to 0.5 mg kg⁻¹ have occurred without causing damage to the plant, while values from 5 to 20 mg kg⁻¹ have been toxic and reduced growth [75]. The As concentrations found in plants grown with and without biochar and mainly treated with biochar are higher than the values considered normal (Table 6). Therefore, this element may have been one of the limiting factors for the growth of this species.

Table 6. Concentration of nutrients and PTEs in *Ipomoea asarifolia*.

	Cu		Mn		Ni mg kg ⁻¹		As		Cr	
	shoot	root	shoot	root	Shoot	root	shoot	root	shoot	Root
SC	5.0 b ± 0.6	16.4 bc ± 0.5	109.9 de ± 12.2	157.6 ab ± 14.0	9.8 bc ± 0.6	47.8 ab ± 3.3	17.1 bc ± 4.3	249.8 c ± 13.9	<LQ	30.7 ab ± 4.7
SM	6.9 b ± 1.8	20.1 ab ± 2.8	169.6 c ± 12.6	175.9 ab ± 28.5	8.3 d ± 0.7	9.5 d ± 0.6	7.6 d ± 2.8	7.3 d ± 1.2	0.0	3.7 c ± 1.2
SC + SM	7.2 b ± 1	17.3 bc ± 1.5	170.2 d ± 58	120.1 b ± 15.6	9.0 bc ± 0.7	34.9 bc ± 2.2	14.9 c ± 3.3	310.3 ab ± 36.3	0.0	24.2 b ± 1.4
SC + SM + BC	9.7 a ± 1.6	16.6 bc ± 1.7	121.0 e ± 33.9	220.2 a ± 21.3	9.3 cd ± 0.4	29.9 c ± 4.4	19.0 bc ± 5.3	255.8 c ± 35.8	0.0	21.8 b ± 4.5
SC + SM + BFe	8.5 a ± 1	16.8 c ± 3.3	193.6 ab ± 26.5	178.2 ab ± 18.6	9.3 b ± 0.3	42.2 abc ± 9.2	14.9 c ± 3.9	266.6 c ± 67.9	<LQ	29.4 ab ± 9.8
SC + BC	8.2 a ± 0.7	20.1 a ± 2.1	214.4 a ± 19.4	162.1 ab ± 21.8	11.4 a ± 0.8	50.9 a ± 5.9	38.7 a ± 5.4	349.5 a ± 44	0.0	48.4 a ± 6.7
SC + BFe	7.5 a ± 1.8	18.7 a ± 4.2	158.7 bc ± 36.6	147.0 b ± 14	31.4 a ± 1.4	47.5 ab ± 10.2	31.5 ab ± 12.8	239.6 bc ± 58.1	0.0	38.2 ab ± 13.9
	Ca		Mg		K mg kg ⁻¹		P		Fe	
	shoot	root	shoot	root	shoot	root	shoot	root	shoot	root
SC	21.9 a ± 1.1	15.7 a ± 0.8	7.4 b ± 0.8	7.9 b ± 1.7	14.4 c ± 1	10.0 d ± 0.3	1.0 d ± 0.1	1.1 d ± 0.1	0.6 b ± 0.1	8.4 a ± 0.4
SM	7.2 b ± 0.8	3.6 f ± 0.3	4.0 c ± 0.3	2.6 d ± 0.1	10.8 d ± 0.7	10.3 d ± 0.6	1.0 d ± 0.1	1.7 bc ± 0.2	0.6 b ± 0.1	4.1 b ± 0.9
SC + SM	19.2 a ± 3.3	6.5 d ± 0.5	11.2 a ± 1.8	12.8 a ± 0.8	11.9 d ± 0.6	13.4 c ± 1.9	1.2 cd ± 0.2	1.3 cd ± 0.1	0.5 b ± 0.2	7.4 a ± 0.3
SC + SM + BC	5.3 c ± 1.1	3.5 f ± 0.03	3.1 d ± 0.3	3.1 d ± 0.2	31.9 a ± 0.3	42.5 a ± 1.6	3.2 a ± 0.5	3.6 a ± 0.6	0.8 ab ± 0.2	6.9 ab ± 0.9
SC + SM + BFe	17.3 a ± 2	8.9 c ± 0.7	8.9 ab ± 0.6	8.1 b ± 0.4	21.7 b ± 1.9	23.5 b ± 2.6	1.6 bc ± 0.1	1.6 bc ± 0.1	0.6 b ± 0.1	9.0 a ± 3.1
SC + BC	7.3 b ± 0.4	4.0 e ± 0.5	3.2 cd ± 0.2	2.7 d ± 0.4	32.5 a ± 2.3	38.3 a ± 3.3	3.0 a ± 0.3	4.5 a ± 0.7	0.8 ab ± 0.1	9.4 a ± 0.9
SC + BFe	20.3 a ± 4.1	12.1 b ± 1.2	7.2 b ± 1.2	5.4 c ± 0.3	19.1 b ± 1.6	26.5 b ± 3.4	1.7 b ± 0.3	2.0 b ± 0.3	1.0 a ± 0.4	8.5 a ± 2.1

Values with the same letter are not significant by the Tukey test ($p < 0.05$). SC = contaminated soil, SM = forest soil, SC + SM = contaminated soil + forest soil, SC + SM + BC = contaminated soil + forest soil + biochar, SC + SM + BFe = contaminated soil + forest soil + biochar Fe impregnated, SC + BC = contaminated soil + biochar, SC + BFe = contaminated soil + biochar Fe impregnated. (mean ± standard deviation). LQ = value below the equipment quantification limit.

3.6. Effect of Biochars on Chlorophyll and Carotenoid Levels

The treatments showed a difference ($p < 0.05$) in relation to the levels of chlorophyll a, b and total, and carotenoids (Figure 5). The treatments with the addition of biochars reduced the photosynthetic pigments. The addition of BC and BFe reduced the total chlorophyll content by 1.5 and twice, respectively, compared to the SC control. Photosynthetic pigments, chlorophylls, and carotenoids are related to the capture of light energy and have been constituted in indicators of environmental stresses in plants, as well as the activity of antioxidant enzymes [8,67,76]. When grown in environments contaminated by PTEs, plants present a series of physiological and nutritional factors, including low concentrations of chlorophylls, carotenoids, and proteins [77].

PTEs with no known function in plants can be absorbed and translocated to the aerial part by the behavior similar to essential elements [78]. For example, As and P have similar ionic behavior and are transported by phosphate-transporting proteins, due to the affinity of these proteins with P [77]. Once present in the plant, As prevents the performance and proper use of P, causing deleterious effects [79]. Li et al. [80] found a reduction of more than 30% in the levels of chlorophyll a, b, and total, and carotenoids, in relation to the control treatment, with an increase in the levels of Cd. Yin et al. [19] observed an increase in the availability of Cd with the addition of 2% BFe. Biochar can solubilize PTEs in the soil, making them bioavailable, increasing absorption by plants [3,59].

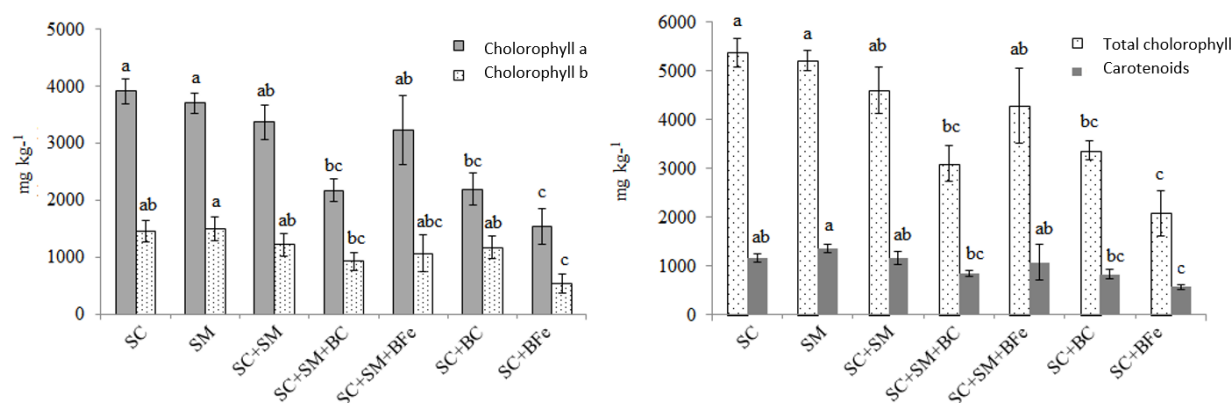


Figure 5. Chlorophyll a, b and total, and carotenoids content after experiment in different treatments. Means followed by the same letter above the bars do not differ statistically from each other by the Tukey test ($p < 0.05$), $n = 4$. Values with the same letter are not significant by the Tukey test ($p < 0.05$). SC = contaminated soil, SM = forest soil, SC + SM = contaminated soil + forest soil, SC + SM + BC = contaminated soil + forest soil + biochar, SC + SM + BFe = contaminated soil + forest soil + biochar Fe impregnated, SC + BC = contaminated soil + biochar, SC + BFe = contaminated soil + biochar Fe impregnated. Mean values with standard deviation bars.

In addition, soil pH and organic matter content (humic acids, fulvic acids, polysaccharides and organic acids) affect the solubility of PTEs [41]. Lomaglio et al. [1] obtained an increase of 70% and 200% in the availability of As and antimony (Sb), respectively, in gold mine soil treated with 5% biochar. Parvez et al. [80] found that As toxicity decreased the content of chlorophyll a, b and total, reduced the cell membrane stability index, and increased the activity of antioxidant enzymes, such as superoxide dismutase, catalase and peroxidase in quinoa (*Chenopodium quinoa Willd.*) plants grown under different doses of As. Inhibition of chlorophyll and carotenoid biosynthesis and reduced phosphorylation are the most frequently observed symptoms of toxicity to PTEs [8]. The reduction in chlorophyll content can be related to the generation of reactive oxygen species with the potential to damage important cell components, such as proteins, nucleic acids, and amino acids involved in chlorophyll biosynthesis [80].

3.7. Distribution of PTEs in Plants

The application of biochars influenced the concentration of PTEs and nutrients in the plants (Table 6). In general, plants cultivated with biochar showed higher concentrations of Cu, Mn, Ni, and As in the aerial part and root. The Mn concentrations were higher in the aerial part in all treatments with biochars, except in SC + SM + BC. Contents of Cr were higher in the roots in all treatments, with emphasis on SC + BC. The nutrients Ca and Mg were less absorbed by plants treated with biochar, mainly in SC + BC, in relation to SC, with K presenting increased absorption.

The addition of BC and BFe to SC increased the concentration of As in the aerial part, by 55 and 46%, respectively, in relation to the control (SC) (Table 6). The concentration of As in the roots increased with the addition of BC to SC; however, for SC + BFe, there was no difference ($p < 0.05$), compared to SC. Regarding the SC + SM mixture, the addition of biochars did not affect the concentration of As in the aerial part, but there was a reduction of 14 and 17% in SC + SM + BFe and SC + SM + BC in the roots.

The increase in the availability of As with the application of non-impregnated biochar was also reported by Lebrun et al. [9] and Lomaglio et al. [6]. The authors attributed the results to the lower adsorption capacity for As compared to positively charged metal ions. In contrast, other studies with biochar impregnated with Fe have reduced the availability of As [19,52]. This was attributed to the success in the impregnation process, in which Fe hydroxides are formed on the surface of biochar, promoting the formation of Fe–O–As (V) complexes. The affinity between Fe and As was suggested and validated as the main

mechanism for sorption of As (V) in Fe hydroxides and consequent reduction of available As [66].

However, even after the impregnation of the açai biochar, the pH of the medium (basic) favored the predominance of negative charges on the surface. Positive and negative charges can coexist on the surface of the biochar, since the pH of the medium has a strong influence on the amount of these charges and, consequently, on the type of contaminant adsorbed (cationic or anionic) [50]. The As concentration observed in the roots of *Ipomoea asarifolia* plants is up to 20 times higher than that found in the leaves. This suggests that the species has the potential to stabilize this element in soils with high As content, in addition to demonstrating that the low translocation may be involved in the stress defense mechanisms of this species.

The increase in As absorption, with the addition of the impregnated biochar, is due to the increase in solubility and some factors that may have contributed to the increase in solubility, which have been discussed previously. There are several mechanisms used by tolerant plants to maintain growth in environments contaminated by PTEs, such as the restriction of absorption in soils with high concentration and translocation to the aerial part [81]. Arsenic is absorbed in the inorganic form of As (V), it is reduced to As (III) and can be complexed by phytochelatins, followed by sequestration in vacuoles [75]. The storage of As (III)-phytochelatin complexes in vacuoles occurs predominantly in the cells of the roots and, to a lesser extent, in the cells of the aerial part [8]. This is an adaptation strategy in rice plants to minimize the translocation of As to the grains [71].

The plants also showed high concentrations of Ni, mainly in the roots (Table 6). Nickel is an essential element for normal plant growth and development. However, Ni toxicity leads to a variety of physiological disorders in plants [82]. The values observed in *Ipomoea asarifolia* plants are in the toxicity range (10 to 100 mg kg⁻¹) [75]. At high concentrations, *Salvinia cucullata* plants resisted excess Cd, Ni, and Mn, mainly by exclusion strategy, in which apparently toxic levels of metals were retained in the root tissues, with minimized translocation to the leaves [83]. For the species *Ipomoea asarifolia*, more studies are important to elucidate the mechanisms of tolerance to As and other PTEs.

3.8. Translocation and Bioconcentration Factors

The translocation factor (TF) was <1 for Ni, Zn, Cd and Pb, regardless of treatment. The TF was >1 for As in SM and Ba in SM and SC + SM, indicating that the low amounts absorbed (approximately 5 mg kg⁻¹ of As in SM and 9 mg kg⁻¹ of Ba in SC + SM) were also translocated, but without characterizing the phytoextraction potential for these elements. The TF for Mn was >1 in SC + SM, SC + SM + BFe, SC + BC and SC + BFe. However, in these treatments, the translocation decreased according to the increase in the absorbed amount, demonstrating that the species has mechanisms that decrease the translocation and thereby minimize the toxic effects of the element.

The bioconcentration factor (BCF) was less than 1 for Ni and As in all treatments (Table 7). Only the SM presented BCF > 1 for Ba, Cd, Pb, Cu, and Mn. These results are consistent with the low levels of SM in relation to the amount absorbed of these elements. The treatments with SM showed BCF > 1 for Zn, due to the reduced amount of PTEs in the soil compared to treatments with only SC, in which the concentration in the soil was higher than that found in the roots. Thus, the values of BCF > 1 and TF < 1 indicated that the species has the potential to phytostabilize Zn, up to certain concentrations in the soil.

Table 7. Translocation and bioconcentration factors in *Ipomoea asarifolia*.

	Translocation Factor							
	Mn	Ni	Zn	As	Ba	Cd	Cu	Pb
SC	0.33	0.20	0.48	0.07	0.33	*	0.31	1.00
SM	0.96	0.87	0.31	1.05	1.28	*	0.34	*
SC + SM	1.42	0.26	0.31	0.05	1.84	*	0.42	*
SC + SM + BC	0.64	0.31	0.64	0.07	0.47	*	0.59	0.10
SC + SM + BFe	1.09	0.22	0.41	0.06	0.82	*	0.51	0.20
SC + BC	1.32	0.22	0.49	0.11	0.06	*	0.41	0.80
SC + BFe	1.08	0.25	0.47	0.13	0.17	0.17	0.40	0.30
	Bioconcentration factor							
	Mn	Ni	Zn	As	Ba	Cd	Cu	Pb
SC	0.31	0.12	0.51	0.07	0.19	0.35	0.10	0.20
SM	5.69	0.63	13.26	0.02	2.84	18.00	4.00	2.80
SC + SM	0.20	0.16	2.40	0.16	0.18	0.96	0.30	0.60
SC + SM + BC	0.26	0.14	1.74	0.15	0.21	0.46	0.30	0.50
SC + SM + BFe	0.28	0.20	1.79	0.16	0.24	0.47	0.30	0.40
SC + BC	0.16	0.14	0.64	0.11	0.47	0.25	0.20	0.20
SC + BFe	0.12	0.12	0.59	0.07	0.54	0.19	0.20	0.20

* Below the limit of quantification in the aerial part.

Some studies have shown that roots are the first barrier to metals, promoting immobilization in the cell wall and extracellular carbohydrates in the rhizosphere, avoiding toxicity in plants [6]. In the roots, metal ions tend to be located in apoplasts, more specifically in cell walls, in which toxic elements are chelated as a result of a defense mechanism against PTEs poisoning, which slows down transport to other plant tissues [84]. In phytostabilization, plants reduce the mobility and availability of pollutants in their environment, immobilizing or preventing migration to other areas of the site [40]. In relation to Mn, TF was greater than 1, but BCF was < 1, therefore it is not classified as phytoextractor.

4. Conclusions

The application of BC in multi-contaminated soil must be carried out with caution, considering the chemical attributes of the soil and characteristics of the PTEs, to avoid the adverse impact on the soil when it is contaminated by As and present high availability of PTEs. Biochars have improved the chemical characteristics of multi-contaminated alkaline soil. The impregnation with Fe used in alkaline soils multi-contaminated by PTEs can increase the immobilization of cations and As in more stable fractions. Considering the bioconcentration and translocation factors, it can be stated that the species *Ipomoea asarifolia* presents potential for the phytostabilization of Zn and is tolerant to As.

Author Contributions: Conceptualization—H.S.C.C., A.R.F., E.S.d.S.; Methodology—H.S.C.C., L.C.A.M., Y.N.D.; Investigation—H.S.C.C., Y.N.D., A.R.F.; Writing—review and editing—H.S.C.C., L.C.A.M., A.R.F. All authors have read and agreed to the published version of the manuscript.

Funding: This work was funded by the National Council for Scientific and Technological Development (CNPq) (N^o.425312/2018-6).

Institutional Review Board Statement: Not applicable.

Informed Consent Statement: Not applicable.

Data Availability Statement: Not applicable.

Acknowledgments: The authors gratefully thank the National Council for Scientific and Technological Development (CNPq) for the financial support (N^o.425312/2018-6) and the Coordination for the Improvement of Higher Education Personnel (Capes) for granting scholarships.

Conflicts of Interest: The authors declare that they have no competing interest.

References

1. Lomaglio, T.; Hattab-Hambli, N.; Bret, A.; Miard, F.; Trupiano, D.; Scippa, G.S.; Motelica-Heino, M.; Bourgerie, S.; Morabito, D. Effect of biochar amendments on the mobility and (bio) availability of As, Sb and Pb in a contaminated mine technosol. *J. Geochem. Explor.* **2017**, *182*, 138–148. [[CrossRef](#)]
2. Midhat, L.; Ouazzani, N.; Hejjaj, A.; Ouhammou, A.; Mandi, L. Accumulation of heavy metals in metallophytes from three mining sites (Southern Centre Morocco) and evaluation of their phytoremediation potential. *Ecotoxicol. Environ. Saf.* **2019**, *169*, 150–160. [[CrossRef](#)] [[PubMed](#)]
3. Souza, E.; Dias, Y.; Costa, H.; Pinto, D.; Oliveira, D.; Falcão, N.; Teixeira, R.; Fernandes, A. Organic residues and biochar to immobilize potentially toxic elements in soil from a gold mine in the Amazon. *Ecotoxicol. Environ. Saf.* **2019**, *169*, 425–434. [[CrossRef](#)] [[PubMed](#)]
4. Souza, E.; Teixeira, R.; Costa, H.; Júnior, F.; Melo, L.; Fernandes, A. Assessment of risk to human health from simultaneous exposure to multiple contaminants in an artisanal gold mine in Serra Pelada. *Sci. Total Environ.* **2017**, *576*, 683–695. [[CrossRef](#)]
5. Mahar, A.; Wang, P.; Ali, A.; Kumar, M.; Hussain, A.; Wang, Q.; Li, R.; Zhang, Z. Challenges and opportunities in the phytoremediation of heavy metals contaminated soils: A review. *Ecotoxicol. Environ. Saf.* **2016**, *126*, 111–121. [[CrossRef](#)]
6. Lomaglio, T.; Hattab-Hambli, N.; Miard, F.; Lebrun, M.; Nandillon, R.; Trupiano, D.; Scippa, G.S.; Gauthier, A.; Motelica-Heino, M.; Bourgerie, S.; et al. Cd, Pb, and Zn mobility and (bio)availability in contaminated soils from a former smelting site amended with biochar. *Environ. Sci. Pollut. Res.* **2017**, *25*, 25744–25756. [[CrossRef](#)]
7. Kabata-Pendias, A. *Trace Elements in Soils and Plants*; CRC Press: Boca Raton, FL, USA, 2010.
8. Bhattacharya, P.; Pal, R. Scope of phytoremediation of Arsenic using *Phormidium tenue* with special reference to modulation in cellular biochemistry. *J. Algal Biomass Util.* **2012**, *3*, 1–8.
9. Lebrun, M.; Macri, C.; Miard, F.; Hattab-Hambli, N.; Motelica-Heino, M.; Morabito, D.; Bourgerie, S. Effect of biochar amendments on As and Pb mobility and phytoavailability in contaminated mine technosols phytoremediated by *Salix*. *J. Geochem. Explor.* **2017**, *182*, 149–156. [[CrossRef](#)]
10. Singh, B.; Macdonald, L.M.; Kookana, R.S.; Zwieten, L.; Butler, G.; Joseph, S. Characterisation and evaluation of biochars for their application as soil amendment Opportunities and constraints for biochar technology in Australian agriculture: Looking beyond carbon sequestration. *Soil Res.* **2014**, *48*, 516–525. [[CrossRef](#)]
11. Lehmann, J.; Gaunt, J. Rondon M Bio-char sequestration in terrestrial ecosystems—A review. *Mitig. Adapt. Strat. Glob. Chang.* **2006**, *11*, 403–427. [[CrossRef](#)]
12. Dias, Y.N.; Souza, E.S.; Costa, H.S.C.; Melo, L.C.A.; Penido, E.S.; Amarante, C.B.; Teixeira, O.M.M.; Fernandes, A.R. Biochar produced from Amazonian agro—industrial wastes: Properties and adsorbent potential of Cd²⁺ and Cu²⁺. *Biochar* **2019**, *1*, 389–400. [[CrossRef](#)]
13. Zama, E.F.; Reid, B.J.; Arp, H.P.H.; Sun, G. Advances in research on the use of biochar in soil for remediation: A review. *J. Soils Sediments* **2018**, *18*, 2433–2450. [[CrossRef](#)]
14. Xu, G.; Lv, Y.; Sun, J.; Shao, H.; Wei, L.; Processes, E.; Key, S.P.; Processes, E. Review Recent Advances in Biochar Applications in Agricultural Soils: Benefits and Environmental Implications. *Clean—Soil Air Water* **2012**, *40*, 1093–1098. [[CrossRef](#)]
15. Ahmad, M.; Lee, S.S.; Lee, S.E.; Al-Wabel, M.I.; Tsang, D.C.W.; Ok, Y.S. Biochar-induced changes in soil properties affected immobilization/mobilization of metals/metalloids in contaminated soils. *J. Soils Sediments* **2017**, *17*, 717–730. [[CrossRef](#)]
16. Wang, B.; Gao, B.; Fang, J. Recent advances in engineered biochar productions and applications. *Crit. Rev. Environ. Sci. Technol.* **2018**, *47*, 2158–2207. [[CrossRef](#)]
17. Rajapaksha, A.U.; Chen, S.S.; Tsang, D.C.W.; Zhang, M.; Vithanage, M. Engineered/designer biochar for contaminant removal/immobilization from soil and water: Potential and implication of biochar modification. *Chemosphere* **2016**, *148*, 276–291. [[CrossRef](#)] [[PubMed](#)]
18. Ahmad, M.; Usman, A.R.A.; Al-Faraj, A.S.; Ahmad, M.; Sallam, A.; Al-Wabel, M.I. Phosphorus-loaded biochar changes soil heavy metals availability and uptake potential of maize (*Zea mays* L.) plants. *Chemosphere* **2018**, *194*, 327–339. [[CrossRef](#)]
19. Yin, D.; Wang, X.; Peng, B.; Tan, C.; Ma, L.Q. Effect of biochar and Fe-biochar on Cd and As mobility and transfer in soil-rice system. *Chemosphere* **2017**, *186*, 928–937. [[CrossRef](#)]
20. Montero, J.I.Z.; Monteiro, A.S.C.; Gontijo, E.S.J.; Bueno, C.C.; Moraes, M.A.; Rosa, A.H. Ecotoxicology and Environmental Safety High efficiency removal of As (III) from waters using a new and friendly adsorbent based on sugarcane bagasse and corn cob husk Fe-coated biochars. *Ecotoxicol. Environ. Saf.* **2018**, *162*, 616–624. [[CrossRef](#)]
21. Ali, H.; Khan, E.; Anwar, M. Phytoremediation of heavy metals—Concepts and applications. *Chemosphere* **2013**, *91*, 869–881. [[CrossRef](#)]
22. Kumar, M.; Seth, A.; Singh, A.K.; Rajput, M.S.; Sikandar, M. Remediation strategies for heavy metals contaminated ecosystem: A review. *Environ. Sustain. Indic.* **2021**, *12*, 100155. [[CrossRef](#)]
23. Wang, L.; Rinklebe, J.; Tack, F.M.G.; Hou, D. A review of green remediation strategies for heavy metal contaminated soil. *Soil Use Manag.* **2021**, *37*, 936–963. [[CrossRef](#)]
24. Thisani, S.K.; von Kallon, D.V.; Byrne, P. Review of remediation solutions for acid mine drainage using the modified hill framework. *Sustainability* **2021**, *13*, 8118. [[CrossRef](#)]

25. Midhat, L.; Ouazzani, N.; Esshaimi, M.; Ouhammou, A.; Mandi, L. Assessment of heavy metals accumulation by spontaneous vegetation: Screening for new accumulator plant species grown in Kettara mine-Marrakech, Southern Morocco. *Int. J. Phytoremediation* **2017**, *19*, 191–198. [[CrossRef](#)] [[PubMed](#)]
26. Midhat, L.; Ouazzani, N.; Hejjaj, A.; Bayo, J.; Mandi, L. Phytostabilization of polymetallic contaminated soil using *Medicago sativa* L. in combination with powdered marble: Sustainable rehabilitation. *Int. J. Phytoremediation* **2018**, *20*, 764–772. [[CrossRef](#)]
27. IBGE. *IBGE Cidades*; Instituto Brasileiro de Geografia e Estatística: Rio de Janeiro, Brazil, 2018.
28. dos Santos, R.N.d.E.S. Investigação do Passivo Ambiental em Cachoeira do Piriá, NE do Pará: Base Para a Gestão Ambiental em Áreas Garimpadas na Amazônia. Ph.D. Thesis, Instituto de Geociências, Universidade de São Paulo, São Paulo, Brazil, 2004. [[CrossRef](#)]
29. Mosher, G.Z. *Technical Report and Resource Estimate on the Cachoeira Property*; Tetra Tech: Pará State, Brazil; Vancouver, DC, USA, 2013; 107p.
30. Klein, E.L.; dos Lopes, E.C.S.; Tavares, F.M.; Campos, L.D.; Souza-Gaia, S.M.; Neves, M.P.; Perrotta, M.M. *Área de Relevante Interesse Mineral: Cinturão do Gurupi*, 23rd ed.; Serviço Geológico do Brasil—CPRM: Brasília, Brazil, 2017; 206p.
31. Lima, A.P.S.; Sarkis, J.E.S.; Shihomatsu, H.M.; Müller, R.C.S. Mercury and selenium concentrations in fish samples from Cachoeira do Piriá Municipality, Pará State, Brazil. *Environ. Res.* **2005**, *97*, 236–244. [[CrossRef](#)]
32. de Neto, H.F.S.; da Pereira, W.V.S.; Dias, Y.N.; de Souza, E.S.; Teixeira, R.A.; de Lima, M.W.; Ramos, S.J.; do Amarante, C.B.; Fernandes, A.R. Environmental and human health risks of arsenic in gold mining areas in the eastern Amazon. *Environ. Pollut.* **2020**, *265*, 114969. [[CrossRef](#)]
33. Teixeira, P.C.; Donagemma, G.K.; Fontana, A.; Teixeira, W.G. (Eds.) *Manual de Metodos de Analise de Solo*, 3rd ed.; Embrapa Solos: Brasília, Brazil, 2017.
34. Pribyl, D.W. Geoderma A critical review of the conventional SOC to SOM conversion factor. *Geoderma* **2010**, *156*, 75–83. [[CrossRef](#)]
35. USEPA; United States Environmental Protection Agency. Microwave Assisted Acid Digestion of Sediments, Sludges, Soils, and Oils. 2007. Available online: <http://www.caslab.com/EPA-Methods/PDF/EPA-Method-3051.pdf> (accessed on 20 October 2021).
36. Song, W.; Guo, M. Journal of Analytical and Applied Pyrolysis Quality variations of poultry litter biochar generated at different pyrolysis temperatures. *J. Anal. Appl. Pyrolysis* **2012**, *94*, 138–145. [[CrossRef](#)]
37. Singh, B.; Camps-Arbestain, M.; Lehmann, J. (Eds.) *Biochar: A Guide to Analytical Methods*; Csiro Publishing: New York, NY, USA, 2017.
38. Uchimiya, M.; Chang, S.; Klasson, K.T. Screening biochars for heavy metal retention in soil: Role of oxygen functional groups. *J. Hazard. Mater.* **2011**, *190*, 432–441. [[CrossRef](#)]
39. Yang, Y.; Chun, Y.; Shang, G.; Huang, M. pH-dependence of pesticide adsorption by wheat-residue-derived black carbon. *Langmuir* **2004**, *20*, 6736–6741. [[CrossRef](#)] [[PubMed](#)]
40. Okoro, J.C.; Saidu, Y.; Anka, S.A. Phytoremediation Potential of *Ipomoea asarifolia* on lead polluted soils. *Bayero J. Pure Appl. Sci.* **2018**, *11*, 301–307. [[CrossRef](#)]
41. Shehu, S.; Wasagu, R.; Anka, S.A.; Okoro, J.C.; Saidu, Y. Phytoremediation of Cadmium-Polluted Soils with *Ipomoea asarifolia* (Desr.) Roem. & Schult. *J. Appl. Sci. Environ. Manag.* **2019**, *23*, 253–259.
42. Zappi, D.C.; Gastauer, M.; Ramos, S.; Nunes, S. *Plantas Nativas Para Recuperação de Áreas de Mineração em Carajás*; Instituto Tecnológico Vale: Belém, PA, USA, 2018.
43. Coringa, J.E.S.; Pezza, L.; Coringa, E.A.O.; Weber, O.L.S. Distribuição geoquímica e biodisponibilidade de metais traço em sedimentos no Rio Bento Gomes, Poconé—MT, Brasil. *Acta Amaz.* **2016**, *46*, 161–174. [[CrossRef](#)]
44. Drahota, P.; Grösslová, Z.; Kindlová, H. Selectivity assessment of an arsenic sequential extraction procedure for evaluating mobility in mine wastes. *Anal. Chim. Acta* **2014**, *839*, 34–43. [[CrossRef](#)]
45. Lichtenthaler, H.K. Chlorophylls Carotenoids: Pigments of photosynthetic biomembranes. *Methods Enzymol.* **1987**, *148*, 350–382.
46. Li, H.; Dong, X.; Evandro, B.; De Oliveira, L.M. Mechanisms of metal sorption by biochars: Biochar characteristics and modifications. *Chemosphere* **2017**, *178*, 466–478. [[CrossRef](#)]
47. Xue, L.; Liu, J.; Shi, S.; Wei, Y.; Chang, E.; Gao, M.; Chen, L.; Jiang, Z. Uptake of Heavy Metals by Native Herbaceous Plants in an Antimony Mine (Hunan, China). *Clean—Soil Air Water* **2014**, *42*, 81–87. [[CrossRef](#)]
48. Melo, L.C.A.; Puga, A.P.; Coscione, A.R.; Beesley, L.; Abreu, C.A.; Camargo, O.A. Sorption and desorption of cadmium and zinc in two tropical soils amended with sugarcane-straw-derived biochar. *J. Soils Sediments* **2015**, *16*, 226–234. [[CrossRef](#)]
49. Han, Z.; Sani, B.; Mroziak, W.; Obst, M.; Beckingham, B.; Karapanagioti, H.K.; Werner, D. Magnetite impregnation effects on the sorbent properties of activated carbons and biochars. *Water Res.* **2014**, *70*, 394–403. [[CrossRef](#)]
50. Borah, D.; Satokawa, S.; Kato, S.; Kojima, T. Sorption of As (V) from aqueous solution using acid modified carbon black. *J. Hazard. Mater.* **2009**, *162*, 1269–1277. [[CrossRef](#)] [[PubMed](#)]
51. Ding, Z.; Xu, X.; Phan, T.; Hu, X.; Nie, G. High adsorption performance for As(III) and As(V) onto novel aluminum-enriched biochar derived from abandoned Tetra Paks. *Chemosphere* **2018**, *208*, 800–807. [[CrossRef](#)] [[PubMed](#)]
52. Wang, S.; Gao, B.; Zimmerman, A.R.; Li, Y.; Ma, L.; Harris, W.G.; Migliaccio, K.W. Removal of arsenic by magnetic biochar prepared from pinewood and natural hematite. *Bioresour. Technol.* **2015**, *175*, 391–395. [[CrossRef](#)] [[PubMed](#)]
53. Wu, C.; Cui, M.; Xue, S.; Li, W.; Huang, L.; Jiang, X.; Qian, Z. Remediation of arsenic-contaminated paddy soil by iron-modified biochar. *Environ. Sci. Pollut. Res.* **2018**, *25*, 20792–20801. [[CrossRef](#)]

54. Gu, Z.; Fang, J.; Deng, B. Preparation and Evaluation of Adsorbents for Arsenic Removal. *Environ. Sci. Technol.* **2005**, *39*, 3833–3843. [[CrossRef](#)]
55. Liao, F.; Yang, L.; Li, Q.; Li, Y.R.; Yang, L.T.; Anas, M.; Huang, D.L. Characteristics and inorganic N holding ability of biochar derived from the pyrolysis of agricultural and forestal residues in the southern China. *J. Anal. Appl. Pyrolysis* **2018**, *134*, 544–551. [[CrossRef](#)]
56. Czaban, J.; Siebielec, G. Effects of bentonite on Sandy soil chemistry in a long-term plot experiment (II); effect on pH, CEC, and macro- and micronutrients. *Pol. J. Environ. Stud.* **2013**, *22*, 1669–1676.
57. Zhang, H.; Chen, C.; Gray, E.M.; Boyd, S.E.; Yang, H.; Zhang, D. Roles of biochar in improving phosphorus availability in soils: A phosphate adsorbent and a source of available phosphorus. *Geoderma* **2016**, *276*, 1–6. [[CrossRef](#)]
58. Zhang, R.H.; Li, Z.-G.; Liu, X.; Wang, B.; Zhou, G.; Huang, X.; Lin, C.; Wang, A.; Brooks, M. Immobilization and bioavailability of heavy metals in greenhouse soils amended with rice straw-derived biochar. *Ecol. Eng.* **2017**, *98*, 183–188. [[CrossRef](#)]
59. Wang, S.; Gao, B.; Li, Y.; Zimmerman, A.R.; Cao, X. Sorption of arsenic onto Ni/Fe layered double hydroxide (LDH)-biochar composites. *RSC Adv.* **2016**, *6*, 17792–17799. [[CrossRef](#)]
60. Fernandes, A.R.; de Souza, E.S.; de Souza Braz, A.M.; Birani, S.M.; Alleoni, L.R.F. Quality reference values and background concentrations of potentially toxic elements in soils from the Eastern Amazon Brazil. *J. Geochem. Explor.* **2018**, *190*, 453–463. [[CrossRef](#)]
61. Conama. Conama-National Council for the Environment, Brazil. 2009; Resolution n° 420/2009. Available online: <http://www.mma.gov.br/port/conama> (accessed on 16 January 2020). (In Portuguese)
62. Kim, M.; Min, H.; Koo, N.; Park, J.; Lee, S.; Bak, G.; Kim, J. The effectiveness of spent coffee grounds and its biochar on the amelioration of heavy metals-contaminated water and soil using chemical and biological assessments. *J. Environ. Manag.* **2014**, *146*, 124–130. [[CrossRef](#)] [[PubMed](#)]
63. Röss, F.; Simonnot, O.M.; Morel, J.L. Short-term effects of biochar on soil heavy metal mobility are controlled by intra-particle diffusion and soil pH increase. *Eur. J. Soil Sci.* **2014**, *65*, 149–161. [[CrossRef](#)]
64. Grygo-szymanko, E.; Tobiasz, A.; Walas, S. Trends in Analytical Chemistry Speciation analysis and fractionation of manganese: A review. *Trends Anal. Chem.* **2016**, *80*, 112–124. [[CrossRef](#)]
65. Bavaresco, J.; Fink, J.R.; Rodrigues, M.L.; Ginanello, C.; Barrón, V.; Torrente, J. Chromium Adsorption in Different Mineralogical Fractions. *Pedosphere* **2017**, *27*, 106–111. [[CrossRef](#)]
66. Puga, A.P.; Melo, L.C.A.; Abreu, C.A.; Coscione, A.R.; Paz-Ferreiro, J. Leaching and fractionation of heavy metals in mining soils amended with biochar. *Soil Tillage Res.* **2016**, *164*, 25–33. [[CrossRef](#)]
67. Zhang, Y.; Fan, J.; Fu, M.; Sik, Y.; Yanwei, O. Adsorption antagonism and synergy of arsenate (V) and cadmium (II) onto Fe-modified rice straw biochars. *Environ. Geochem. Health* **2017**, *41*, 1755–1766. [[CrossRef](#)]
68. Chen, F.; Wang, S.; Mou, S.; Azimuddin, I.; Zhang, D.; Pan, X.; Al-misned, F.A.; Mortuza, M.G. Physiological responses and accumulation of heavy metals and arsenic of *Medicago sativa* L. growing on acidic copper mine tailings in arid lands. *J. Geochem. Explor.* **2015**, *157*, 27–35. [[CrossRef](#)]
69. Tang, J.; Zhu, W.; Kookana, R.; Katayama, A. Characteristics of biochar and its application in remediation of contaminated soil. *J. Biosci. Bioeng.* **2013**, *116*, 653–659. [[CrossRef](#)]
70. Rodríguez-Vila, A.; Asensio, V.; Forján, R.; Covelo, E.F. Chemical fractionation of Cu, Ni, Pb and Zn in a mine soil amended with compost and biochar and vegetated with *Brassica juncea* L. *J. Geochem. Explor.* **2015**, *158*, 74–81. [[CrossRef](#)]
71. Feng, Y.; Liu, P.; Wang, Y.; Finfrook, Y.Z.; Xie, X.; Su, C.; Liu, N.; Yang, Y.; Xu, Y. Distribution and speciation of iron in Fe-modified biochars and its application in removal of As(V), As(III), Cr(VI), and Hg(II): An X-ray absorption study Yu. *J. Hazard. Mater.* **2019**, *384*, 121342. [[CrossRef](#)] [[PubMed](#)]
72. Suriyagoda, L.D.B.; Dittert, K.; Lambers, H. Arsenic in Rice Soils and Potential Agronomic Mitigation Strategies to Reduce Arsenic Bioavailability: A Review. *Pedosphere* **2018**, *28*, 363–382. [[CrossRef](#)]
73. Beesley, L.; Inneh, O.S.; Norton, G.J.; Moreno-Jimenez, E.; Pardo, T.; Clemente, R.; Dawson, J.J. Assessing the influence of compost and biochar amendments on the mobility and toxicity of metals and arsenic in a naturally contaminated mine soil. *Environ. Pollut.* **2014**, *186*, 195–202. [[CrossRef](#)] [[PubMed](#)]
74. Silva, J.R.I.; Jardim, A.L.F.; Neto, J.B.; Leite, M.L.M.V.; Teixeira, V.I. Estresse salino como desafio para produção de plantas forrageiras. *Pesqui. Apl. Agrotecnol.* **2018**, *11*, 127–139. [[CrossRef](#)]
75. Pandey, C.; Augustine, R.; Panthri, M.; Zia, I.; Bisht, N.C.; Gupta, M. Plant Physiology and Biochemistry Arsenic affects the production of glucosinolate, thiol and phytochemical compounds: A comparison of two Brassica cultivars. *Plant Physiol. Et Biochem.* **2017**, *111*, 144–154. [[CrossRef](#)]
76. Demarco, C.F.; Afonso, T.F.; Pieniz, S. Phytoremediation of heavy metals and nutrients by the *Sagittaria montevidensis* into an anthropogenic contaminated site at Southern of Brazil. *Int. J. Phytoremediation* **2019**, *21*, 1145–1152. [[CrossRef](#)]
77. Yadav, K.; Gupta, N.; Kumar, A.; Reece, L.; Singh, N.; Rezanian, S.; Ahmad, S. Mechanistic understanding and holistic approach of phytoremediation: A review on application and future prospects. *Ecol. Eng.* **2018**, *120*, 274–298. [[CrossRef](#)]
78. Suriyagoda, L.D.B.; Dittert, K.; Lambers, H. Mechanism of arsenic uptake, translocation and plant resistance to accumulate arsenic in rice grains Agriculture, Ecosystems and Environment Mechanism of arsenic uptake, translocation and plant resistance to accumulate arsenic in rice grains. *Agric. Ecosyst. Environ.* **2018**, *253*, 23–37. [[CrossRef](#)]

79. Rehman, M.Z.; Rizwan, M.; Ali, S.; Fatima, N.; Yousaf, B.; Naeem, A.; Sabir, M.; Raza, H.; Sik, Y. Contrasting effects of biochar, compost and farm manure on alleviation of nickel toxicity in maize (*Zea mays* L.) in relation to plant growth, photosynthesis and metal uptake. *Ecotoxicol. Environ. Saf.* **2016**, *133*, 218–225. [[CrossRef](#)]
80. Parvez, S.; Abbas, G.; Shahid, M.; Amjad, M.; Hussain, M.; Ahmad, S.; Imran, M.; Asif, M. Effect of salinity on physiological, biochemical and photostabilizing attributes of two genotypes of quinoa (*Chenopodium quinoa* Willd.) exposed to arsenic stress. *Ecotoxicol. Environ. Saf.* **2020**, *187*, 109814. [[CrossRef](#)]
81. Das, S.; Mazumdar, K. Phytoremediation potential of a novel fern, *Salvinia cucullata*, Roxb. Ex Bory, to pulp and paper mill effluent: Physiological and anatomical response. *Chemosphere* **2016**, *163*, 62–72. [[CrossRef](#)] [[PubMed](#)]
82. Finnegan, P.M.; Chen, W. Arsenic toxicity: The effects on plant metabolism. *Front. Physiol.* **2012**, *3*, 182. [[CrossRef](#)] [[PubMed](#)]
83. Abbas, G.; Murtaza, B.; Bibi, I.; Shahid, M.; Niazi, N.K.; Khan, M.I.; Amjad, M.; Hussain, M.; Natasha. Arsenic uptake, toxicity, detoxification, and speciation in plants: Physiological, biochemical, and molecular aspects. *Int. J. Environ. Res. Public Health* **2018**, *15*, 59. [[CrossRef](#)] [[PubMed](#)]
84. Li, X.; Zhao, M.; Guo, L.; Huang, L. Effect of cadmium on photosynthetic pigments, lipid peroxidation, antioxidants, and artemisinin in hydroponically grown *Artemisia annua*. *J. Environ. Sci.* **2012**, *24*, 1511–1518. [[CrossRef](#)]